AMERICAN SOCIETY FOR MICROBIOLOGY | mBio®

RESEARCH ARTICLE
Therapeutics and Prevention

Efficacy of Oral Encochleated Amphotericin B in a Mouse Model of Cryptococcal Meningoencephalitis

R. Lu,[a] C. Hollingsworth,[b] J. Qiu,[b] A. Wang,[c] E. Hughes,[c] X. Xin,[c] K. M. Konrath,[c] W. Elsegeiny,[b] Yoon-Dong Park,[b] L. Atakulu,[b] J. C. Craft,[a] E. C. Tramont,[d] R. Mannino,[a] P. R. Williamson[b]

[a]Matinas BioPharma, Bedminster, New Jersey, USA
[b]Laboratory of Clinical Immunology and Microbiology, National Institute of Allergy and Infectious Diseases, National Institutes of Health, Bethesda, Maryland, USA
[c]National Center for Advancing Translational Sciences, National Institutes of Health, Rockville, Maryland, USA
[d]Division of Clinical Research, National Institute of Allergy and Infectious Diseases, National Institutes of Health, Bethesda, Maryland, USA

ABSTRACT *Cryptococcus neoformans* is an encapsulated yeast responsible for approximately a quarter of a million deaths worldwide annually despite therapy, and upwards of 11% of HIV/AIDS-related deaths, rivaling the impact of tuberculosis and malaria. However, the most effective antifungal agent, amphotericin B, requires intravenous delivery and has significant renal and hematopoietic toxicity, making it difficult to utilize, especially in resource-limited settings. The present studies describe a new nanoparticle crystal encapsulated formulation of amphotericin B known as encochleated amphotericin B (CAmB) that seeks to provide an oral formulation that is low in toxicity and cost. Using a 3-day delayed model of murine cryptococcal meningoencephalitis and a large inoculum of a highly virulent strain of serotype A *C. neoformans*, CAmB, in combination with flucytosine, was found to have efficacy equivalent to parental amphotericin B deoxycholate with flucytosine and superior to oral fluconazole without untoward toxicity. Transport of fluorescent CAmB particles to brain as well as significant brain levels of amphotericin drug was demonstrated in treated mice, and immunological profiles were similar to those of mice treated with conventional amphotericin B. Additional toxicity studies using a standardized rat model showed negligible toxicity after a 28-day treatment schedule. These studies thus offer the potential for an efficacious oral formulation of a known fungicidal drug against intrathecal cryptococcal disease.

IMPORTANCE *Cryptococcus neoformans* is a significant global fungal pathogen that kills an estimated quarter of a million HIV-infected individuals yearly and has poor outcomes despite therapy. The most effective therapy, amphotericin B, is highly effective in killing the fungus but is available only in highly toxic, intravenous formulations that are unavailable in most of the developing world, where cryptococcal disease in most prevalent. For example, in Ethiopia, reliance on the orally available antifungal fluconazole results in high mortality, even when initiated as preemptive therapy at the time of HIV diagnosis. Thus, alternative agents could result in significant saving of lives. Toward this end, the present work describes the development of a new formulation of amphotericin B (CAmB) that encapsulates the drug as a crystal lipid nanoparticle that facilitates oral absorption and prevents toxicity. Successful oral absorption of the drug was demonstrated in a mouse model that, in combination with the antifungal flucytosine, provided efficacy equal to a parental preparation of amphotericin B plus flucytosine. These studies demonstrate the potential for CAmB in combination with flucytosine to provide an effective oral formulation of a well-known, potent fungicidal drug combination.

KEYWORDS *Cryptococcus*, amphotericin, clinical therapeutics, fungus

Citation Lu R, Hollingsworth C, Qiu J, Wang A, Hughes E, Xin X, Konrath KM, Elsegeiny W, Park Y-D, Atakulu L, Craft JC, Tramont EC, Mannino R, Williamson PR. 2019. Efficacy of oral encochleated amphotericin B in a mouse model of cryptococcal meningoencephalitis. mBio 10:e00724-19. https://doi.org/10.1128/mBio.00724-19.

Editor Gary B. Huffnagle, University of Michigan Medical School

Address correspondence to P. R. Williamson, williamsonpr@mail.nih.gov.

R.L. and C.H. contributed equally to this work.

This article is a direct contribution from a Fellow of the American Academy of Microbiology. Solicited external reviewers: Stuart Levitz, University of Massachusetts Medical School; Tom Kozel, Univ Nevada.

Received 20 March 2019
Accepted 16 April 2019
Published 28 May 2019

Cryptococcus neoformans is an encapsulated yeast responsible for between a quarter of a million and a half million deaths annually (1, 2), rivaling the mortality of tuberculosis and malaria. However, despite these grim statistics, the most effective pharmaceutical agent for this disease, amphotericin B deoxycholate (Fungizone), remains a difficult-to-administer intravenous (i.v.), toxic medication developed in the 1950s (3, 4). Other fungicidal agents such as oral (p.o.) fluconazole have poor outcomes approaching 100% mortality in standard-dose regimens, thought to be due to their fungistatic mechanism, rather than the fungicidal mechanism of amphotericin B (3, 5). However, the toxicities and exclusive i.v. formulations of amphotericin B require sophisticated electrolyte monitoring and intravenous catheters that have precluded use of this medication in a significant number of countries in the African continent with large populations at risk (www.gaffi.org). Even preemptive therapy for *C. neoformans* disease at the time of HIV diagnosis results in up to 70% mortality when oral azole therapy is utilized (6). The result of these poor therapeutics and diagnostics has been a continued silent epidemic of mortality (7).

New formulations of amphotericin B, including a novel encochleated form, seek to provide a formulation that is both orally available and of low toxicity and cost (8). Preparations of these lipid nanoparticles are unique in that they have an anhydrous core that releases the incorporated drug formulation in a calcium-dependent fashion, facilitating intracellular drug delivery (8). Such a preparation could open up the prospect of the potent fungicidal activity of amphotericin-based therapeutics for cryptococcal disease to the developing world. However, challenges remain to determine if the drug can be delivered in effective concentrations to the brain, where the most severe *C. neoformans* infections occur. Thus, in the present study, various formulations of encochleated amphotericin B (CAmB) were administered to mice via intraperitoneal (i.p.) and subcutaneous (s.c.) injections, as well as by oral gavage. Adjunctive flucytosine (5FC) was also mixed into the drinking water of groups of mice in combination with oral CAmB as 5FC is a known anticryptococcal fungicidal preparation having demonstrated synergy with amphotericin B (9). In these studies, multiple formulations of CAmB were evaluated to test which compound and route of administration were most efficient against *C. neoformans* in mice. A delayed-treatment model that results in more rapid failure of fungistatic drugs such as fluconazole than of fungicidal amphotericin B was also utilized (10).

RESULTS

Oral-dose CAmB protects mice against infection with *C. neoformans*. ND4 mice were infected intravenously with 10^4 CFU of a highly virulent strain of *C. neoformans* followed with either amphotericin B deoxycholate (5 mg/kg of body weight/day) intraperitoneally (i.p.) or CAmB orally in the indicated doses and then followed until moribund. As shown in Fig. 1A, a 1-day delay in initiating therapy resulted in protection versus untreated controls with either the systemically administered ($P < 0.001$) or oral ($P < 0.01$) CAmB with sterilization of brains in 9 of 10 animals in both groups. In contrast, in a discovery study of multiple formulations, a 3-day delay in therapy (Fig. 1B) resulted in reduced efficacy of all drugs tested, allowing discrimination of median survivals between the fungistatic drug fluconazole (53 days, $P < 0.002$ versus untreated), monotherapy with 5FC (47 days, $P < 0.002$ versus untreated), and a high-dose amphotericin B regimen previously described to be effective in a mouse model (10) in combination with 5FC (11). Using this model, CAmB at 5 mg/kg/day i.p. or 25 mg/kg/day orally resulted in prolongation of survival versus controls (49 and 35 days, versus 19 days, $P < 0.003$ and $P < 0.003$, respectively), and addition of 5FC to oral CAmB achieved survival comparable to that of the amphotericin B-5FC combination (102 versus 80 days, $P = 0.5$). Additional amphotericin B formulations were assessed for efficacy (see Fig. S1 in the supplemental material), but all were equivalent to the CAmB formulation. Subsequently, a larger group experiment was conducted to further confirm the survival similarity between oral CAmB and the conventional AmB combination regimen using the delayed-treatment model. While some variation in mortality was expected due to

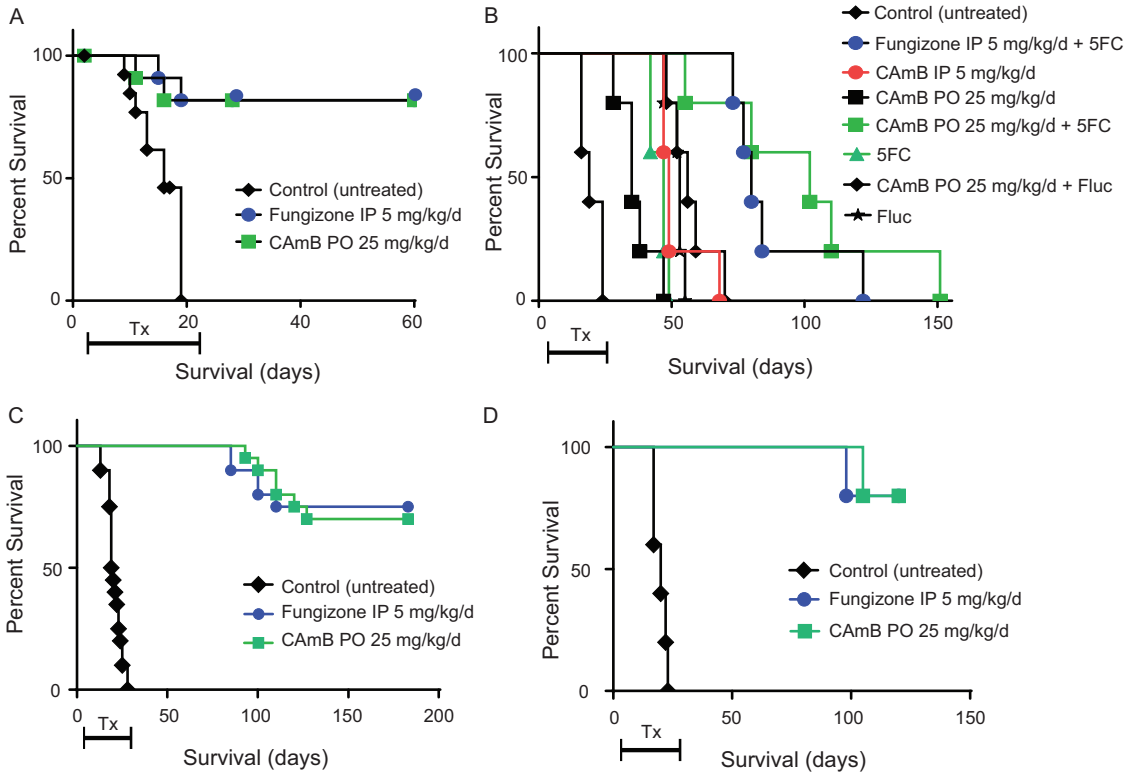

FIG 1 An encochleated oral formulation of amphotericin B (CAmB) protects against a highly virulent strain of *C. neoformans* in a delayed-treatment model. (A) Ten mice were inoculated intravenously with 10^4 CFU of *C. neoformans* and, after 24 h, were treated for 20 days with either amphotericin B, i.p. 5 mg/kg/day, or CAmB, p.o. 50 mg/kg/day, and followed until moribund. (B) Five mice in each group were inoculated as in panel A, treated with the indicated formulations at the indicated doses for 28 days, and followed until moribund. (C and D) Twenty female mice (C) or 5 male mice (D) were inoculated as in panel B, treated as indicated above, and followed for mortality.

slight differences in fungal viability or variations in host response of the outbred ND4 mouse strain, mortality was similar using either regimen (CAmB + 5FC, $P < 0.01$ versus untreated; amphotericin B + 5FC, $P = 0.012$ versus untreated), resulting in 70% survival in both groups in female mice (Fig. 1C). Because *C. neoformans* disease demonstrates gender differences in prevalence as well as outcome (12), we also conducted experiments in male mice which again demonstrated equivalence between the CAmB oral combination regimen and the parental AmB regimen (Fig. 1D; CAmB + 5FC, $P < 0.002$ versus untreated; amphotericin B + 5FC, $P = 0.002$ versus untreated). Brain and lung cultures of all surviving mice showed an absence of fungal CFU (<10 CFU/g tissue), suggesting effective microbiologic control with either regimen.

Oral CAmB results in effective brain clearance of *C. neoformans*. The same mouse model as in Fig. 1B was used to examine rates of fungal clearance from brains of mice, since in humans rates of intrathecal clearance of organisms are a prognostic factor of clinical outcome during therapy (3, 5, 13). As shown in Fig. 2, the 3-day-delay model resulted in high brain fungal burdens in both treated groups. However, amphotericin B i.p. reduced brain fungal load after 9 to 11 daily doses versus untreated controls (median fungal load over 9 to 11 doses, 4×10^3 CFU/g versus 5.4×10^5 CFU/g; $P < 0.01$), with slightly smaller but still significant reductions achieved with the oral CAmB versus the untreated control (1.7×10^4 CFU/g, $P < 0.01$).

Oral CAmB results in levels of amphotericin B comparable to parental amphotericin B. As shown in Fig. 3A and Tables 1 and 2, there was little accumulation in serum between doses 15, 17, and 19 with a slight increase in brain levels in the amphotericin B-treated mice. Given the relative constancy in drug levels during the last week of the 3-week treatment course, data were pooled among the last three dose time points

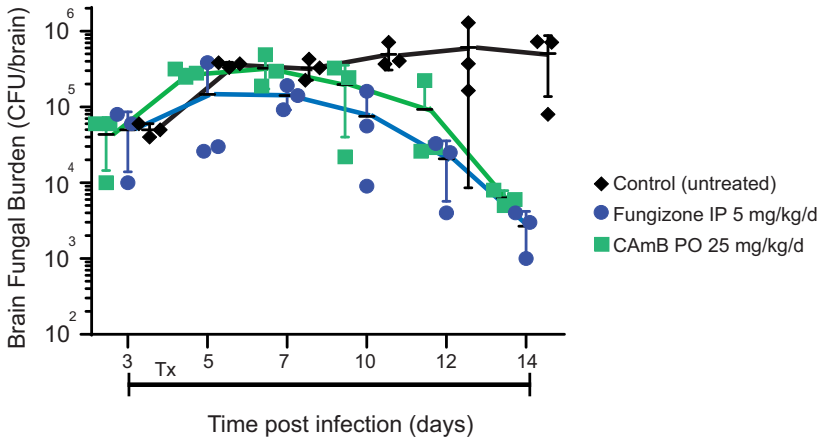

FIG 2 Treatment with an encochleated oral formulation of CAmB results in reductions in brain fungal burden in a *C. neoformans* delayed-treatment model. Mice were treated as in Fig. 1B above with the indicated formulations and sacrificed after the indicated number of treatments, and brain fungal burden was determined. $n = 3$ for each group; error bars show ±SD.

which were observed for steady-state amphotericin B levels. Oral CAmB resulted in average detectable levels of amphotericin B on days 15, 17, and 19 at 1 h posttreatment (795 ± 542 ng/ml, ± SD, $n = 10$) comparable to those achieved with amphotericin B at 5 mg/kg/day i.p. (697± 323 ng/ml, ± SD, $n = 10$). Average levels increased at 6 h after each dose with each preparation and were higher with the amphotericin B preparation (CAmB, 790 ± 184 ng/ml, ± SD, $n = 10$; amphotericin B, 1,197 ± 368 ng/ml, ± SD, $n = 3$; $P < 0.01$). Average brain levels 6 h after dosing on day 19 were also significant in the CAmB-treated group, although higher levels were achieved in the amphotericin B-treated mice (CAmB, 218 ± 43.4 ng/g, ± SD, $n = 10$, versus amphotericin B, 394 ± 32 ng/g, ± SD, $n = 10$; $P < 0.05$). To further characterize brain penetration by the cochleate amphotericin, a preparation of CAmB was labeled with a fluorescent tag to allow visualization by fluorescence microscopy. As shown in Fig. 3B, the orally absorbed CAmB was taken up in brains of intact mice and visualized in infected mice. Interestingly, little fluorescence was visualized in brains of uninfected mice, consistent with a dependence on an infected milieu for effective tissue penetration. Within infected brains, fluorescent CAmB particles were not detected within brain-infiltrating monocytes by flow cytometry (Fig. S2), suggesting a lack of persistent cellular residence of CAmB during drug delivery and retention within the intrathecal space.

Oral CAmB treatment of mice results in similar inflammatory cytokine changes in lung as conventional amphotericin B. Previous studies have demonstrated that amphotericin B results in induction of cytokines, including TNF-α, IL-1β, and IL-6, and chemokines CCL2 and CCL4 in peritoneal macrophages through a TLR2-dependent mechanism (14). Since the inflammatory milieu may influence survival (15–21), we asked if amphotericin B treatment resulted in detectable changes in the lung cytokine and chemokine milieu and if CAmB altered these relationships by assessing lung homogenates after short-term treatment with these pharmaceuticals. After infection, mice were treated with the same amphotericin B preparations as in Fig. 1B but without 5FC, and then lungs were harvested and assayed for cytokine levels after either one or two drug treatments. As shown in Fig. 4, in the absence of amphotericin B, infection with *Cryptococcus neoformans* resulted in significant increases in IL-6 (126 versus 5 pg/lung; $P < 0.05$), CCL2 (1,200 versus 47 pg/lung; $P < 0.05$), and CCL4 (median, 93 versus 25 pg/lung; $P = 0.02$) and a trend toward increased median lung cytokine levels of IL-1β (55 versus 23 pg/lung; $P = 0.06$), compared to uninfected controls. TNF-α increased somewhat but was also not statistically significant versus untreated controls (100 versus 41 pg/lung; $P = 0.19$). Treatment of infected animals resulted in slight increases in median IL-1β levels that were statistically significant only after the first dose

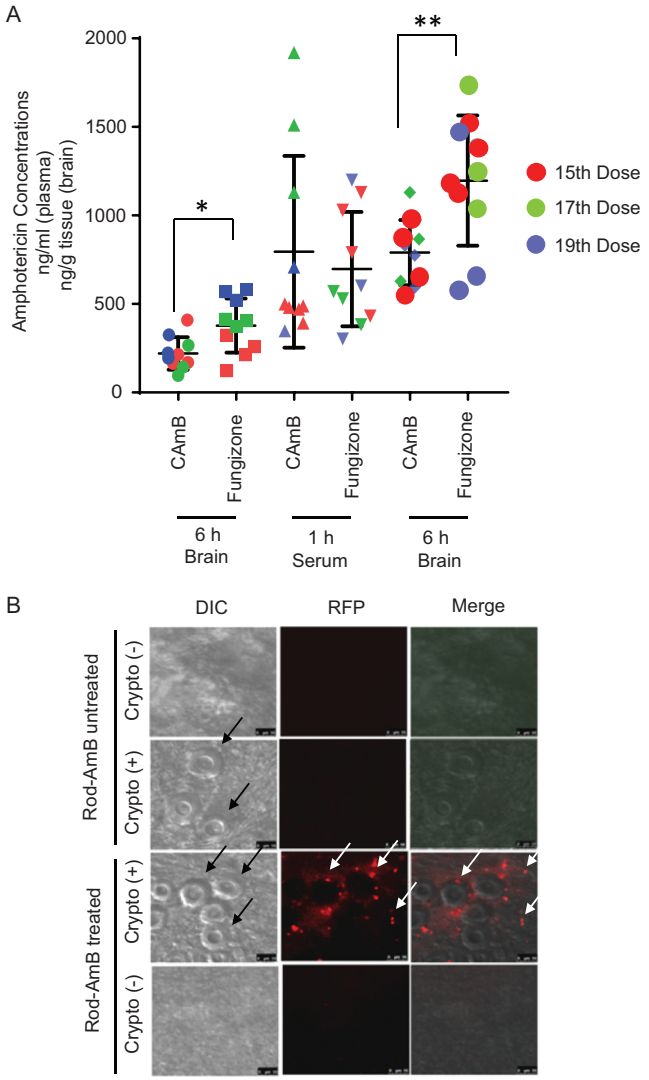

FIG 3 Treatment with an encochleated oral formulation of CAmB results in accumulation of amphotericin B in brains of *C. neoformans*-infected mice. (A) Mice were infected as in Fig. 1B above and treated with the indicated formulations of amphotericin B. After the indicated doses of each formulation, serum was obtained 1 h after dosing, serum and brains were harvested at 6 h from sacrificed animals, and amphotericin B concentrations were determined by HPLC-MS as described in Materials and Methods ($n = 9$ animals; *, $P < 0.05$; **, $P < 0.01$; error bars, ±SD). (B) Mice were infected intravenously with 10^4 CFU of *C. neoformans* [Crypto (+)] or remained uninfected [Crypto (-)]. Five days later, mice were treated daily for 3 days with fluorescent CAmB (Rod-AmB) p.o. and sacrificed. Brains were removed, homogenized, and subjected to microscopy using differential interference contrast (DIC) or fluorescence microscopy (RFP). Black arrows show *C. neoformans*, and white arrows show CAmB fluorescent puncta. Bar, 5 μm.

of CAmB (92 versus 55 pg/lung; $P < 0.05$). However, treatment with both amphotericin formulations resulted in modest reductions in IL-6 levels in lungs of mice which were statistically significant after CAmB (median, 22 versus 126 pg/lung; $P < 0.05$) and were persistent for both preparations at the second dose (median, amphotericin B, 11 versus 126 pg/lung [$P < 0.05$]; CAmB, 13 versus 126 pg/lung [$P < 0.05$]). Modest reductions after treatment with either formulation were also present in CCL2 as well as CCL4 of infected animals, which became significant for both preparations after the second dose (CCL2, amphotericin B, 358 versus 1,200 pg/lung, $P < 0.05$; CAmB, 347 versus 1,200 pg/lung, $P < 0.05$; CCL4, amphotericin B, 64 versus 93 pg/lung, $P < 0.05$; CAmB, 65 versus 1,200 pg/lung, $P < 0.05$). In contrast, TNF-α levels showed little change after treatment with either preparation.

TABLE 1 Blood plasma levels of amphotericin B delivered by cochleate p.o. or deoxycholate i.p.[a]

Formulation and time posttreatment (h)	Mean level (ng/ml) ± SD (*n*) at treatment day(s):			
	Day 15	Day 17	Day 19	Days 15–19
CAmB, p.o., 25 mg/kg/day				
1	461 ± 47	1,520 ± 395	515 ± 181	795 ± 542
6	770 ± 197 (4)	875 ± 251 (3)	733 ± 123 (3)	790 ± 184 (10)
AmB, i.p., 5 mg/kg/day				
1	846 ± 310	494 ± 99	702 ± 457	697 ± 323
6	1,308 ± 180 (4)	1,343 ± 359 (3)	902 ± 494 (3)	1,197 ± 368 (10)

[a]A 3-week steady-state experiment was performed to observe the accumulation of amphotericin B in the plasma of mice associated with either CAmB p.o. or AmB i.p. administration. Mice were dosed according to weight for a period of 3 weeks, and blood samples were taken at days 15, 17, and 19 at 1 h posttreatment and 6 h posttreatment.

Twenty-eight-day oral-dose treatment of rats with CAmB results in no discernible weight loss or hematological, organ, or histological damage compared to vehicle control-treated animals. Efficacy studies in mice resulted in no discernible toxicities in the CAmB treatment group compared to those treated with conventional amphotericin B plus 5FC, evidenced by equivalent weights at the end of treatment in either female or male mice (Fig. 5A). However, to better identify and characterize potential toxicities of CAmB, a standardized 28-day oral-dose toxicity study was undertaken utilizing the Sprague-Dawley rat model with both male and female animals. Briefly, three groups of 24 female and 24 male rats were treated with either 30 mg/kg/day, 45 mg/kg/day, or 90 mg/kg/day of CAmB, compared to a group pf 15 female and 15 male rats treated with vehicle control, respectively, and followed for daily weights. All animals survived, except for the early deaths of three animals. These animals were examined at necropsy and determined to have died from barotrauma as the result of the gavage procedure. In surviving animals, neither female (Fig. 5B, left panel) nor male (Fig. 5B, right panel) rats displayed significant differences in weight at day 29 after completion of treatment, compared to the control group. In addition, absolute organ weights did not differ between treatment and vehicle control groups in either males (Table S1) or females (Table S2).

Hematological and clinical chemistry findings. Absolute monocytes (AMO) and the percentage of monocytes (PMO) in the white blood cells (WBC) decreased in some males in the medium- and high-dose groups compared with the controls on day 29 at interim sacrifice (Table S3), but not in females (Table S4). However, on day 42, AMO and PMO were increased in the high-dose group in males, and associated white blood cells (WBC) were increased in the medium- and high-dose groups. The changes were thus thought to be due to individual sporadic changes in the control group and not related to the treatment with CAmB. Sporadic changes were seen in the males of treated groups on day 29, including an increase in platelet counts (PLC) in the low-dose group and decreases in the reticulocyte counts (REA) and in the ratios of reticulocytes to red blood cells (RET) in the high-dose group. None of the changes showed dose depen-

TABLE 2 Brain levels of amphotericin B delivered by cochleate p.o. or deoxycholate i.p.[a]

Formulation	Mean level (ng/ml) ± SD (*n*) at treatment day(s):			
	Day 15	Day 17	Day 19	Days 15–19
CAmB, p.o., 25 mg/kg/day	239 ± 115 (4)	168 ± 88 (3)	247 ± 69 (3)	218 ± 43.4 (10)
AmB, i.p., 5 mg/kg/day	229 ± 84 (4)	397 ± 22 (3)	557 ± 32 (3)	394 ± 164 (10)

[a]Mice were subjected to a 3-week steady-state study to observe steady-state brain levels of amphotericin B after sustained treatment. Brain samples were collected 6 h posttreatment on days 15, 17, and 19.

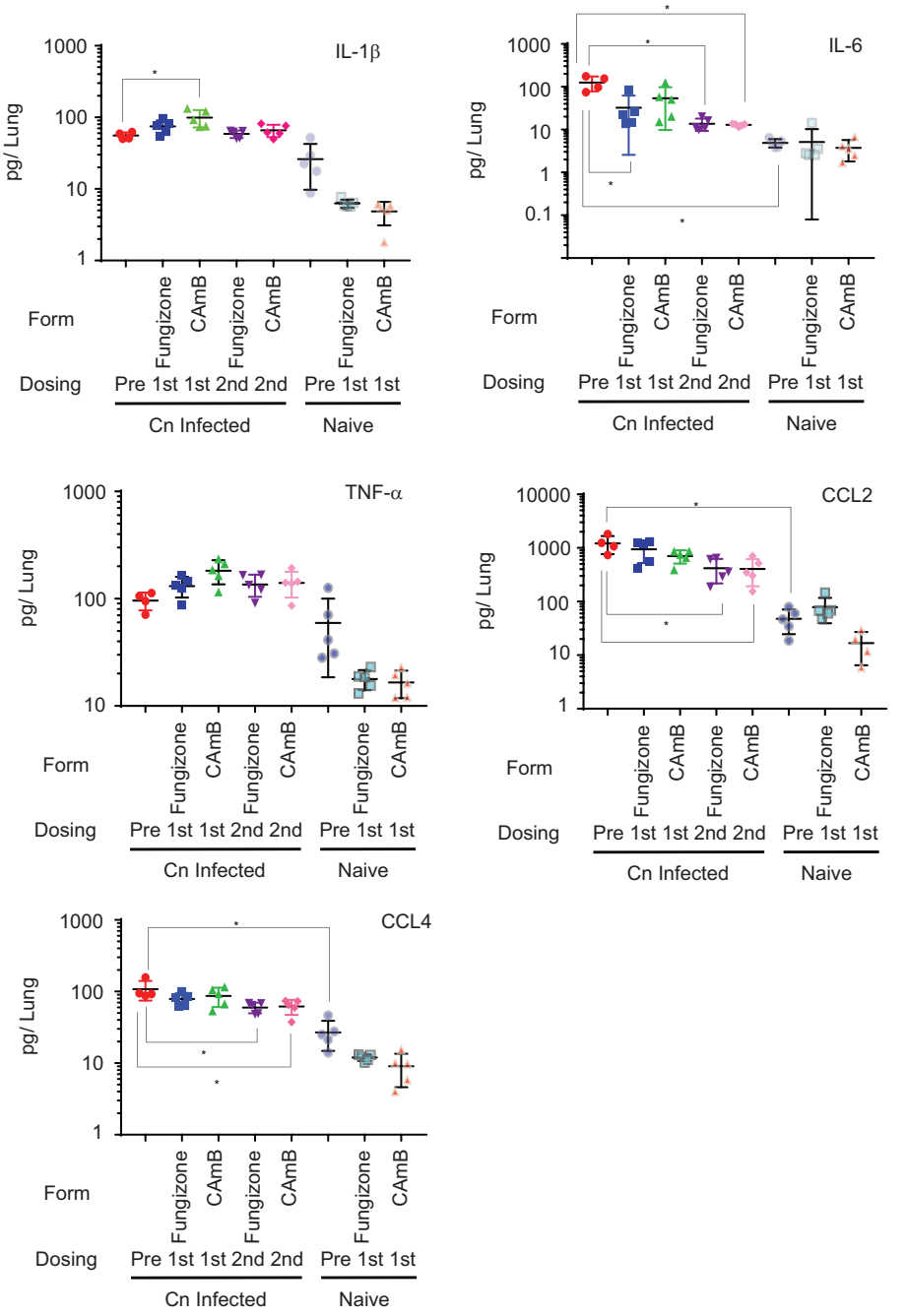

FIG 4 Treatment with an encochleated oral formulation of CAmB results in a similar cytokine milieu as that after treatment with amphotericin B in lungs of *C. neoformans*-infected mice. Groups of mice were inoculated as in Fig. 1B, after 1 week (Cn Infected) were treated with the indicated formulation daily (without 5FC), and were sacrificed after the indicated doses, and lung homogenates were assayed for the indicated cytokines. Uninfected mice served as controls (naive). $n = 5$ mice per group; *, $P < 0.05$; error bars, ±SD.

dency. On day 42, a slight but statistically significant increase was seen in red blood cell distribution width (RDW) in the males of the high-dose group compared with males in the control group. No changes were seen in the female rats at day 29 and day 42 terminal sacrifices after 2 weeks of recovery. The changes in hematology parameters were felt to represent spontaneous changes and were not considered to be related to the test article administration.

Serum sodium, chloride, and calcium concentrations showed small changes in males that were dose dependent (Table S5) and that were not evident in the females

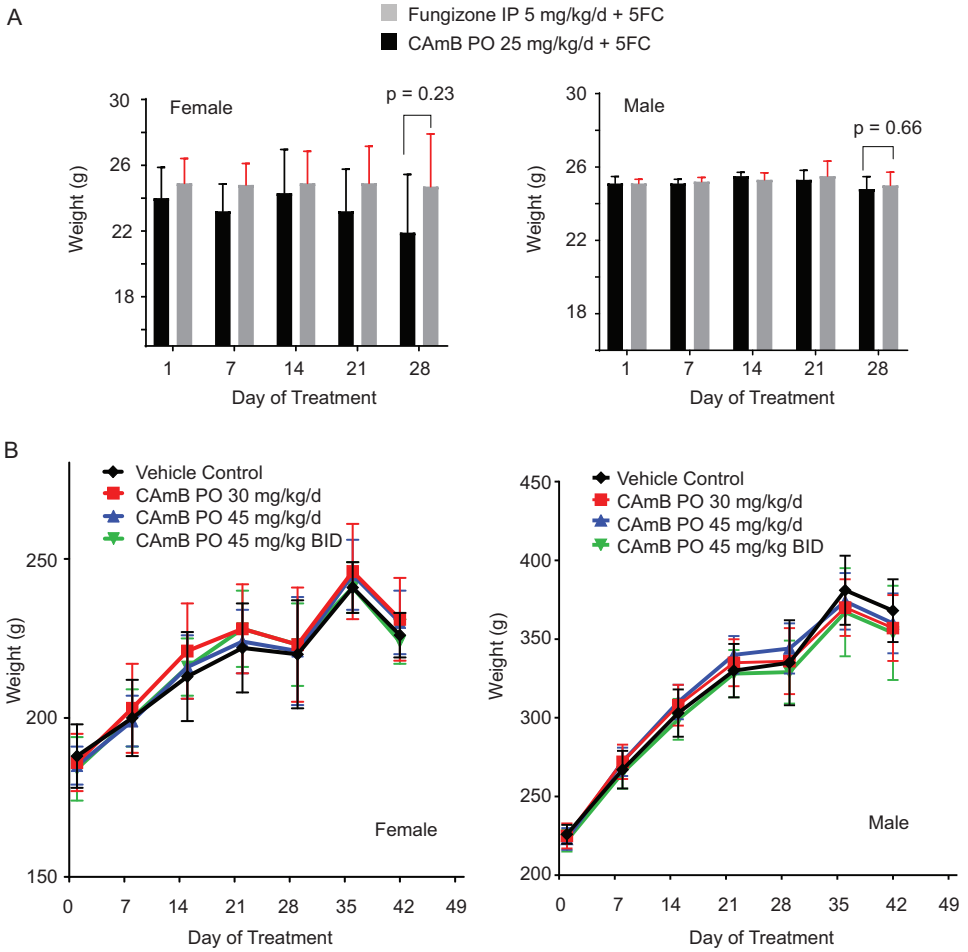

FIG 5 Treatment with oral CAmB shows no discernible weight loss in mice or rats compared to treatment with amphotericin B. (A) *C. neoformans*-infected female (left panel) or male (right panel) mice (in experiments described in the Fig. 1C and D legend) were each given the indicated doses of CAmB p.o. or amphotericin B i.p. plus 5FC, weights were obtained daily, and weights on indicated days are shown. Weights at the end of therapy on day 28 were compared ($n = 13$ for each group; female, $P = 0.23$; male, $P = 0.66$). (B) Uninfected female (left panel) or male (right panel) rats were treated with the indicated doses of CAmB p.o. ($n = 5$ per group ± SD). BID, twice daily.

(Table S6). Sporadic changes in phosphorus and CO_2 were also evident in males, as was an alkaline phosphatase elevation in females that was not dose dependent.

Gross necropsy findings. Several grossly observable abnormalities were noted in both control and/or test article-treated groups in the following tissues: lung with bronchi, thymus, mandibular lymph nodes, spleen, adrenal glands, liver, kidney, ovaries, uterus, and heart. Discolored or mottled lungs and discolored mandibular lymph nodes were found frequently in both the control and the treated groups. These findings were most likely terminal/agonal effects secondary to euthanasia. More red, discolored ovaries were noted in the females of the high-dose group (5 of 15 females) than in the controls (2 of 15 females); however, no abnormal pathology was observed on microscopic evaluations.

Histological findings. Tissues collected from animals in the control and high-dose groups as well as animals with an unscheduled death or that were euthanized in a moribund condition or tissues with significant gross findings at the time of processing or necropsy were evaluated microscopically by the pathologist. Findings for rats that received vehicle control or CAmB were not distributed in a manner suggesting adverse effect at either the interim necropsy on day 29 or the terminal necropsy after 2 weeks of recovery on day 42. All microscopic findings noted were related to spontaneous disease or conditions or to terminal necropsy procedures. All other necropsy findings

were minor, infrequent, and inconsistent and were regarded as incidental background changes unrelated to the test article. In conclusion, no discernible differences were observed in blood analysis, urinalysis, or organ histologies between the CAmB-treated animals and the vehicle control.

DISCUSSION

The present studies are the first to demonstrate oral delivery of the potent fungicidal amphotericin B to the intrathecal compartment, potentially useful for CNS fungal infections. Unlike lipidation, encochleation results in a central anhydrous core within a lipid-containing crystal nanoparticle that is more stable to degradation until subjected to a calcium-poor intracellular environment. This results in successful oral uptake and therapeutic levels of drug available to be delivered to distant tissues, including the CNS. Based on previous studies, six formulations of CAmB were tested in a mouse model of cryptococcal meningitis designed to maximize the potential for drug failure that utilized a highly virulent *Cryptococcus grubii* strain (H99) and a 3-day delay before initiation of therapy (10). In this model, mice succumb to a CNS infection with high brain fungal burdens, similar to that in human HIV-related infections (22). This model resulted in failure of the fungistatic drug fluconazole, similar to that seen in human infections (3). Flucytosine (5FC), a fungicidal drug not recommended as monotherapy for cryptococcal meningoencephalitis (CM) in human infections, was effective in combination with amphotericin B i.p. given at 5 mg/kg/day in combination with 5FC as previously described (11) and is the recommended regimen in human infections (23).

In combination with 5FC, CAmB given by oral gavage was as effective as the parental amphotericin B plus 5FC using moribundity as an endpoint in both studies of 5 female mice each and larger samples of 20 mice. Clearance of brain fungal burden was also similar to that of the parental amphotericin B combination regimen. Brain fungal clearance, measured by rates of fungal load in cerebrospinal fluid, is an important microbiological surrogate of antifungal activity in human patients (3, 13, 24). In addition, since males predominate in the numbers of cryptococcal infections in the United States (12), we tested the combination CAmB plus 5FC in male mice to test gender as a biological variable. Similarly to that previously reported in mice, mortality was similar between untreated male and female mice (25), and equivalent efficacy of the oral CAmB combination was also gender independent, which may reduce concerns of gender-specific therapeutic outcomes in patients raised by some investigators based on data including differing immunosuppressive effects of sex hormones (26).

Examination of tissue drug delivery took account of the unique attributes of amphotericin B. While absolute levels of amphotericin B can vary tremendously in plasma and tissue between preparations that have similar efficacies and thus may have limited predictive value by themselves (27), we assessed plasma and tissue levels of amphotericin B at the oral 25-mg/kg/day dose of CAmB plus 5FC to provide a rough blood surrogate of treatment efficacy associated with mouse moribundity. Recognizing these caveats, we measured "steady-state" brain levels and serum levels of amphotericin in mice which did not vary significantly from each other after the 15th, 17th, or 19th dose. In addition, while serum levels 6 h after dosing showed a higher value after amphotericin B dosing than oral CAmB, brain levels did not show significant differences, consistent with the equivalent efficacy in the CM model. Interestingly, using a rhodamine-tagged CAmB preparation, microscopy of the brains of mice demonstrated intrathecal delivery of the nanoparticles and potentiation by the cryptococcal infection. However, we were not able to demonstrate specific cellular localization of the fluorescent signal using flow cytometry. This could be due to lysis of the transporting macrophage after egress into the CNS or a cell-independent mechanism of intrathecal delivery such as transcytosis (28).

Another important variable affecting patient outcomes may be immune dysregulations that could either reduce microbial clearance or result in inflammatory syndromes, similar to cryptococcal immune reconstitution inflammatory syndrome (cIRIS) after antiretroviral therapy (ART) in HIV-related disease or a postinfectious inflammatory

syndrome in non-HIV patients (15, 29, 30) which is also present during murine infections (31). In the present study, CAmB treatment in the presence of CM resulted in small but significant elevations in IL-1β, the proinflammatory cytokine that had previously been reported to be elevated after exposure to conventional AmB (14, 32). However, TNF-α did not show significant changes after CAmB treatment in infected animals, and IL-6 showed small reductions, in contrast to large increases demonstrated in previous studies using older formulations of AmB (33, 34). Such inflammatory reactions have been related to AmB-related liposome impurities, resulting in toxicities such as fever and renal toxicity (35, 36), and may help to explain the absence of observed toxicity with CAmB, similar to other nanoparticle delivery formulations (37). More inflammation-neutral preparations may thus help to reduce inflammatory syndromes such as cIRIS or postinfectious inflammatory response syndrome (PIIRS) in these patients, potentially improving outcome.

Toxicity of amphotericin preparations remains the principal limiting property of current formulations. No observable toxicity was observed in mice after treatment with the combination of CAmB and 5FC as evidenced by equivalent weights in the treatment groups. However, to allow more generalization of toxicity data, a standard multidose (28-day) rat toxicity model was utilized consistent with regulatory requirements. In these studies, all animals survived except for 3 early deaths of three animals attributed to barotrauma from the oral gavage. The remainder of the animals displayed no overt toxicity effects at a dose up to 90 mg/kg/day, above that given to the mice in efficacy models. These studies were conducted in both male and female animals, again suggesting no gender-dependent difference as a biological variable in the use of these preparations. Indeed, CAmB has been recently studied in a phase II efficacy study in patients with chronic azole-resistant mucocutaneous candidiasis without evident toxicity (38).

In summary, these studies demonstrate the utility of an orally available encochleated form of amphotericin B, CAmB, which in combination with 5FC shows promising efficacy in a murine model of cryptococcal meningoencephalitis. These studies also demonstrate the ability of encochleated formulations to deliver therapeutic levels of pharmaceuticals by an oral route to the CNS. Follow-on human studies in patients with CM are planned.

MATERIALS AND METHODS

Fungal strains, plasmids, and growth media. The *C. neoformans* ATCC 208821 (H99) strain was a gift from J. Perfect. Strains were grown in YPD agar containing 2% glucose, 1% yeast extract, and 2% Bacto peptone. ND4 mice were obtained from Envigo.

CAmB and vehicle control formulations. The lipid nanoparticle used for amphotericin drug delivery and rhodamine-labeled AmB cochleate was formulated according to the method of Santangelo et al. (8). Briefly, a basic solution of amphotericin B (22.75 g, Sigma) in 0.1 N NaOH (707 ml) is added, dropwise with stirring, to an aqueous suspension of liposomes (106 g lipoid PS P50X in 3.533 liters of 50 mM phosphate buffer, pH 7.4), followed by the addition, dropwise with stirring, of calcium chloride (1.0 M, 194.8 ml) to form the CAmB suspension containing 1.8 mg AmB/ml. The final formulation step involves removal of supernatant followed by addition of methylcellulose (0.3%) as a suspending agent with adjustment to a final concentration of 5 mg AmB/ml. Preparations of CAmB-S were made in the same way, but CAmB was sonicated in a Branson 1510 water bath sonicator for 10 min at 0°C. CAmB-S Deoxy was prepared by sonicating CAmB plus 2 mM deoxycholate (Sigma). CAmB-S-BSA was prepared by sonicating CAmB plus 10 mg/ml bovine serum albumin (Sigma). CAmB-S-FAT was made by sonicating CAmB plus 0.45 g milk fat, and CAmB 2.5:1 was prepared using 50% less lipoid PS P50X.

Infection model. An intravenous mouse model described previously was utilized (10, 39). Briefly, ND4 wild-type (WT) mice were inoculated intravenously with 10^4 fungal cells grown on YPD agar. The viability of the inoculum was determined as greater than 90% by assessing CFU on YPD agar. After 24 h (Fig. 1A) or 72 h (Fig. 1B), treatment with the indicated compounds was begun and continued for 20 days (Fig. 1A) or 28 days (Fig. 1B). Mice were then followed until moribund and were sacrificed, and their brains were cultured for CFU.

Measurement of steady-state levels of amphotericin B: animals and grouping. Eighty-one ND4 mice were divided into three different treatment groups consisting of 27 animals each: CAmB treated, AmB treated, and untreated. All 81 animals were infected with *C. neoformans* as described above, and the respective treatments began 3 days after inoculation. Amphotericin B at 5 mg/kg daily was given i.p. (group 1), CAmB at 25 mg/kg daily (group 2) was given by oral gavage, and flucytosine was given to groups 1 and 2 at an estimated dose of 250 mg/kg daily based on an oral consumption of 4 ml daily as described above and was adjusted based on mouse weights (11). Groups 1 and 2 were treated daily for

a period of 3 weeks, and after the indicated doses, 3 mice from each group were sacrificed and brains were collected to measure CFU. To assess steady-state amphotericin levels, blood and brain samples were collected after the indicated doses to determine steady-state plasma and brain levels of amphotericin B. Blood samples were collected 1 h and 6 h posttreatment using the mandibular bleed technique. Blood was collected in EDTA-treated collection tubes. Brain samples were taken at 6 h posttreatment and weighed upon retrieval. A section of brain was removed from each sample and homogenized for assessing fungal burden. The remaining section of brain was weighed again before homogenization in 3 volumes of deionized, sterile water for amphotericin B level analysis.

Determination of amphotericin B concentrations in mouse plasma and brain samples. Plasma samples were harvested from blood collected in EDTA tubes. After brain tissue collection, the tissue sample was rinsed with cold saline, dried on filtrate paper, and weighed. The weight of each tissue was recorded and snap-frozen by placement on dry ice. Three volumes of water was added to brain tissue and then homogenized. Ten microliters of plasma and 40 μl of tissue homogenate were added to 200 μl of internal standard (100 ng/ml tolbutamide in acetonitrile-methanol, 6:4) in a 96-well plate to precipitate proteins. The plate was vortexed for 5 min and centrifuged at 3,000 rpm for 30 min at 4°C. The supernatant was collected and stored at −80°C until analysis.

An ultrahigh-performance liquid chromatography–tandem mass spectrometry (UPLC-MS/MS) method was developed and optimized to determine amphotericin B concentrations in plasma and brain homogenate samples. Briefly, mass spectrometric analysis was performed on a Waters Xevo TQ-S triple-quadrupole instrument using electrospray ionization in positive mode with selected reaction monitoring (SRM). The most intense SRM of amphotericin B was the protonated dehydrated AmB *m/z* 906.6 to *m/z* 743.5. The separation was performed on an Acquity BEH C_{18} column (50 by 2.1 mm, 1.7 μm) using a Waters Acquity UPLC system with an 0.6-ml/min flow rate. The column temperature was maintained at 60°C. Mobile phase A was 0.1% formic acid in water, and mobile phase B was 0.1% formic acid in acetonitrile. The UPLC gradient method was 2% B (0 to 0.2 min), 2% B to 95% B (0.2 to 1.2 min), 95% B (1.2 to 1.8 min), and 2% B (1.8 to 2.0 min). The retention time of amphotericin B was 1.0 min. The total run time was 2 min. With the optimized UPLC-MS/MS method, the peak width of amphotericin B was ~2 s, which increased resolution and reduced potential endogenous interference. The calibration standards (10 to 5,000 ng/ml) were prepared in the control blank mouse plasma and brain homogenate. A 1.0-μl supernatant was injected for the UPLC-MS/MS analysis.

Flow cytometry analysis of rhodamine-labeled CAmB. Two mice were infected with 100 μl of 10^4 CFU of *C. neoformans* (H99), and one mouse remained naive. One of the infected mice received 200 μl of the rhodamine-labeled, encochleated amphotericin B p.o. once a day (SID) for 2 days. This treatment took place 1 week postinfection. Animals were euthanized on day 3 posttreatment via isoflurane overdose. Mice were then perfused through the left ventricle using 12 ml of cold PBS in a syringe with a 22-gauge needle. The perfused brains were subsequently removed. Each brain was placed in 5 ml of RPMI using an 8-well plate. Each brain was minced and was passed through a 70-μm filter. Filtrate was washed in RPMI, then mixed with 33.3% Percoll-RPMI suspension, and then centrifuged for 30 min at 800 × g (no brake) to allow separation of monocytes. Isolated monocytes were then counted and prepared for fluorescence-activated cell sorting (FACS) analysis. Cells were stained for $CD31^+$, $CD45^+$, and $Ly6C^+$ populations. After staining, cells were fixed using the BD Cytofix/PermWash kit for 20 min and then washed using BD PermWash. Cells remained in PermWash buffer during FACS analysis.

Cytokine protein measurements. Cytokine levels in lung tissues were analyzed using the Bio-Plex protein array system (Luminex-based technology; Bio-Rad Laboratories, Hercules, CA) according to the manufacturer's directions. Briefly, lung tissue was excised and homogenized in ice-cold, sterile PBS (1 ml) and kept on ice. An aliquot (10 μl) was taken to quantify the pulmonary fungal burden, and an antiprotease buffer solution (1 ml) containing PBS, protease inhibitors (inhibiting cysteine, serine, and other metalloproteinases), and 0.05% Triton X-100 was added to the homogenate, which was then clarified by centrifugation (800 × *g*) for 5 min.

Twenty-eight-day oral-dose toxicity study in Sprague-Dawley rats. The study was performed in accordance with reference 40 under NIAID contract no. HHSN2662007000043C/NO1-AI-70043, protocol study number M573-08. Briefly, four groups of rats were treated with either 30 mg/kg/day (24 males, 24 females), 45 mg/kg/day (24 males, 24 females), or 90 mg/kg/day (24 males, 24 females) of CAmB or a vehicle control (15 males, 15 females) and monitored with daily weighings. On day 29, 20 rats (10 males, 10 females) from each group were selected. Animals were subjected to fasting before blood collection. Blood was collected from the retro-orbital sinus under 60:40% CO_2-O_2 anesthesia before necropsy on days 29 and 49 for main and recovery groups, respectively. Hematology parameters, including hemoglobin and red blood cell and white blood cell counts with differential evaluation, were measured. Complete serum chemistry was also evaluated, including blood urea nitrogen, alanine aminotransferase, creatinine, and bilirubin. Animals were euthanized using an overdose of sodium pentobarbital administered by intraperitoneal injection. For necropsy and histopathological examinations, all tissues from all control and high-dose animals and those tissues deemed necessary by the pathologist (e.g., tissue observed to have significant gross findings) were examined. Sections of the tissues were embedded in paraffin, were cut approximately 5 μm thick, and underwent H&E staining. A four-step grading system (minimal, mild, moderate, and marked) was used to define gradable lesions for comparison between the treated and control groups. Records of gross findings for a specimen from postmortem observations were available to the pathologist when examining specimens microscopically.

Statistics. Errors were expressed as standard deviation (SD). Statistical significance of mouse survival times was assessed by log rank (Mantel-Cox test). Discovery studies (Fig. 1A and B; see also Fig. S1 in the supplemental material) were not adjusted for multiple comparisons, but important relationships were

confirmed with focused studies (Fig. 1B and C) in both female and male mice. Comparison of fungal burdens, drug levels, and cytokines in the respective tissue or in serum was performed by a nonparametric *t* test with Welch's correction. Plots were made and statistical analysis was performed using GraphPad Prism version 5.0a (GraphPad Software, San Diego, CA, USA).

SUPPLEMENTAL MATERIAL

Supplemental material for this article may be found at https://doi.org/10.1128/mBio.00724-19.

FIG S1, EPS file, 2.1 MB.
FIG S2, PDF file, 1.1 MB.
TABLE S1, DOCX file, 0.02 MB.
TABLE S2, DOCX file, 0.02 MB.
TABLE S3, DOCX file, 0.02 MB.
TABLE S4, DOCX file, 0.02 MB.
TABLE S5, DOCX file, 0.02 MB.
TABLE S6, DOCX file, 0.02 MB.

ACKNOWLEDGMENTS

This research was supported by the Intramural Research Program of the NIH, NIAID, and a Cooperative Research and Development Agreement (CRADA) from Matinas BioPharma.

REFERENCES

1. Park BJ, Wannemuehler KA, Marston BJ, Govender N, Pappas PG, Chiller TM. 2009. Estimation of the current global burden of cryptococcal meningitis among persons living with HIV/AIDS. AIDS 23:525–530. https://doi.org/10.1097/QAD.0b013e328322ffac.
2. Rajasingham R, Smith R, Park B, Jarvis J, Govender NP, Chiller T, Denning D, Loyse A, Boulware DR. 2017. Global burden of disease of HIV-associated cryptococcal meningitis: an updated analysis. Lancet Infect Dis 17:873–881. https://doi.org/10.1016/S1473-3099(17)30243-8.
3. Bicanic T, Meintjes G, Wood R, Hayes M, Rebe K, Bekker L, Harrison T. 2007. Fungal burden, early fungicidal activity, and outcome in cryptococcal meningitis in antiretroviral-naive or antiretroviral-experienced patients treated with amphotericin B or fluconazole. Clin Infect Dis 45:76–80. https://doi.org/10.1086/518607.
4. Baddley JW, Forrest GN, AST Infectious Diseases Community of Practice. 2013. Cryptococcosis in solid organ transplantation. Am J Transplant 13(Suppl 4):242–249. https://doi.org/10.1111/ajt.12116.
5. Bicanic T, Muzoora C, Brouwer AE, Meintjes G, Longley N, Taseera K, Rebe K, Loyse A, Jarvis J, Bekker LG, Wood R, Limmathurotsakul D, Chierakul W, Stepniewska K, White NJ, Jaffar S, Harrison TS. 2009. Independent association between rate of clearance of infection and clinical outcome of HIV-associated cryptococcal meningitis: analysis of a combined cohort of 262 patients. Clin Infect Dis 49:702–709. https://doi.org/10.1086/604716.
6. Beyene T, Zewde AG, Balcha A, Hirpo B, Yitbarik T, Gebissa T, Rajasingham R, Boulware DR. 2017. Inadequacy of high-dose fluconazole monotherapy among cerebrospinal fluid cryptococcal antigen (CrAg)-positive human immunodeficiency virus-infected persons in an Ethiopian CrAg screening program. Clin Infect Dis 65:2126–2129. https://doi.org/10.1093/cid/cix613.
7. Adams P. 4 January 2016. How to stop crypto, a deadly disease so neglected it's missed on the 'neglected' list. Newsweek. http://www.newsweek.com/2016/01/15/crushing-crypto-world-health-organization-neglected-disease-411193.html.
8. Santangelo R, Paderu P, Delmas G, Chen ZW, Mannino R, Zarif L, Perlin DS. 2000. Efficacy of oral cochleate-amphotericin B in a mouse model of systemic candidiasis. Antimicrob Agents Chemother 44:2356–2360. https://doi.org/10.1128/AAC.44.9.2356-2360.2000.
9. Dromer F, Bernede-Bauduin C, Guillemot D, Lortholary O, French Cryptococcosis Study Group. 2008. Major role for amphotericin B-flucytosine combination in severe cryptococcosis. PLoS One 3:e2870. https://doi.org/10.1371/journal.pone.0002870.
10. Graybill JR, Mitchell L, Levine HB. 1978. Treatment of experimental murine cryptococcosis: a comparison of miconazole and amphotericin B. Antimicrob Agents Chemother 13:277–283. https://doi.org/10.1128/AAC.13.2.277.
11. Schwarz P, Dromer F, Lortholary O, Dannaoui E. 2006. Efficacy of amphotericin B in combination with flucytosine against flucytosine-susceptible or flucytosine-resistant isolates of Cryptococcus neoformans during disseminated murine cryptococcosis. Antimicrob Agents Chemother 50:113–120. https://doi.org/10.1128/AAC.50.1.113-120.2006.
12. Pyrgos V, Seitz AE, Steiner CA, Prevots DR, Williamson PR. 2013. Epidemiology of cryptococcal meningitis in the US: 1997-2009. PLoS One 8:e56269. https://doi.org/10.1371/journal.pone.0056269.
13. Montezuma-Rusca JM, Powers JH, Follmann D, Wang J, Sullivan B, Williamson PR. 2016. Early fungicidal activity as a candidate surrogate endpoint for all-cause mortality in cryptococcal meningitis: a systematic review of the evidence. PLoS One 11:e0159727. https://doi.org/10.1371/journal.pone.0159727.
14. Sau K, Mambula SS, Latz E, Henneke P, Golenbock DT, Levitz SM. 2003. The antifungal drug amphotericin B promotes inflammatory cytokine release by a Toll-like receptor- and CD14-dependent mechanism. J Biol Chem 278:37561–37568. https://doi.org/10.1074/jbc.M306137200.
15. Meya DB, Okurut S, Zziwa G, Rolfes MA, Kelsey M, Cose S, Joloba M, Naluyima P, Palmer BE, Kambugu A, Mayanja-Kizza H, Bohjanen PR, Eller MA, Wahl SM, Boulware DR, Manabe YC, Janoff EN. 2015. Cellular immune activation in cerebrospinal fluid from Ugandans with cryptococcal meningitis and immune reconstitution inflammatory syndrome. J Infect Dis 211:1597–1606. https://doi.org/10.1093/infdis/jiu664.
16. Bahr NC, Wallace J, Frosch AE, Boulware DR. 2014. Unmasking cryptococcal meningitis immune reconstitution inflammatory syndrome due to granulocyte colony-stimulating factor use in a patient with a poorly differentiated germ cell neoplasm. Case Rep Oncol 7:1–5. https://doi.org/10.1159/000357666.
17. Haddow LJ, Colebunders R, Meintjes G, Lawn SD, Elliott JH, Manabe YC, Bohjanen PR, Sungkanuparph S, Easterbrook PJ, French MA, Boulware DR, International Network for the Study of HIV-Associated IRIS (INSHI). 2010. Cryptococcal immune reconstitution inflammatory syndrome in HIV-1-infected individuals: proposed clinical case definitions. Lancet Infect Dis 10:791–802. https://doi.org/10.1016/S1473-3099(10)70170-5.
18. Jarvis JN, Meintjes G, Bicanic T, Buffa V, Hogan L, Mo S, Tomlinson G, Kropf P, Noursadeghi M, Harrison TS. 2015. Cerebrospinal fluid cytokine profiles predict risk of early mortality and immune reconstitution inflammatory syndrome in HIV-associated cryptococcal meningitis. PLoS Pathog 11:e1004754. https://doi.org/10.1371/journal.ppat.1004754.
19. Jarvis JN, Casazza JP, Stone HH, Meintjes G, Lawn SD, Levitz SM, Harrison TS, Koup RA. 2013. The phenotype of the Cryptococcus-specific CD4+ memory T-cell response is associated with disease severity and outcome

in HIV-associated cryptococcal meningitis. J Infect Dis 207:1817–1828. https://doi.org/10.1093/infdis/jit099.
20. McKinney C, Merriman ME, Chapman PT, Gow PJ, Harrison AA, Highton J, Jones PB, McLean L, O'Donnell JL, Pokorny V, Spellerberg M, Stamp LK, Willis J, Steer S, Merriman TR. 2008. Evidence for an influence of chemokine ligand 3-like 1 (CCL3L1) gene copy number on susceptibility to rheumatoid arthritis. Ann Rheum Dis 67:409–413. https://doi.org/10.1136/ard.2007.075028.
21. Parayath KE, Harrison TS, Levitz SM. 2000. Effect of interleukin (IL)-15 priming on IL-12 and interferon-gamma production by pathogen-stimulated peripheral blood mononuclear cells from human immunodeficiency virus-seropositive and -seronegative donors. J Infect Dis 181:733–736. https://doi.org/10.1086/315280.
22. Williamson PR, Jarvis JN, Panackal AA, Fisher MC, Molloy SF, Loyse A, Harrison TS. 2017. Cryptococcal meningitis: epidemiology, immunology, diagnosis and therapy. Nat Rev Neurol 13:13–24. https://doi.org/10.1038/nrneurol.2016.167.
23. Saag MS, Graybill RJ, Larsen RA, Pappas PG, Perfect JR, Powderly WG, Sobel JD, Dismukes WE. 2000. Practice guidelines for the management of cryptococcal disease. Infectious Diseases Society of America. Clin Infect Dis 30:710–718. https://doi.org/10.1086/313757.
24. Loyse A, Wilson D, Meintjes G, Jarvis JN, Bicanic T, Bishop L, Rebe K, Williams A, Jaffar S, Bekker LG, Wood R, Harrison TS. 2012. Comparison of the early fungicidal activity of high-dose fluconazole, voriconazole, and flucytosine as second-line drugs given in combination with amphotericin B for the treatment of HIV-associated cryptococcal meningitis. Clin Infect Dis 54:121–128. https://doi.org/10.1093/cid/cir745.
25. Lortholary O, Improvisi L, Fitting C, Cavaillon JM, Dromer F. 2002. Influence of gender and age on course of infection and cytokine responses in mice with disseminated Cryptococcus neoformans infection. Clin Microbiol Infect 8:31–37. https://doi.org/10.1046/j.1469-0691.2002.00375.x.
26. Furman D, Hejblum BP, Simon N, Jojic V, Dekker CL, Thiebaut R, Tibshirani RJ, Davis MM. 2014. Systems analysis of sex differences reveals an immunosuppressive role for testosterone in the response to influenza vaccination. Proc Natl Acad Sci U S A 111:869–874. https://doi.org/10.1073/pnas.1321060111.
27. Lestner JM, Howard SJ, Goodwin J, Gregson L, Majithiya J, Walsh TJ, Jensen GM, Hope WW. 2010. Pharmacokinetics and pharmacodynamics of amphotericin B deoxycholate, liposomal amphotericin B, and amphotericin B lipid complex in an in vitro model of invasive pulmonary aspergillosis. Antimicrob Agents Chemother 54:3432–3441. https://doi.org/10.1128/AAC.01586-09.
28. Patel MM, Patel BM. 2017. Crossing the blood-brain barrier: recent advances in drug delivery to the brain. CNS Drugs 31:109–133. https://doi.org/10.1007/s40263-016-0405-9.
29. Sungkanuparph S, Filler SG, Chetchotisakd P, Pappas PG, Nolen TL, Manosuthi W, Anekthananon T, Morris MI, Supparatpinyo K, Kopetskie H, Kendrick AS, Johnson PC, Sobel JD, Larsen RA. 2009. Cryptococcal immune reconstitution inflammatory syndrome after antiretroviral therapy in AIDS patients with cryptococcal meningitis: a prospective multicenter study. Clin Infect Dis 49:931–934. https://doi.org/10.1086/605497.
30. Panackal AA, Wuest SC, Lin YC, Wu T, Zhang N, Kosa P, Komori M, Blake A, Browne SK, Rosen LB, Hagen F, Meis J, Levitz SM, Quezado M, Hammoud D, Bennett JE, Bielekova B, Williamson PR. 2015. Paradoxical immune responses in non-HIV cryptococcal meningitis. PLoS Pathog 11:e1004884. https://doi.org/10.1371/journal.ppat.1004884.
31. Neal LM, Xing E, Xu J, Kolbe JL, Osterholzer JJ, Segal BM, Williamson PR, Olszewski MA. 2017. CD4(+) T cells orchestrate lethal immune pathology despite fungal clearance during Cryptococcus neoformans meningoencephalitis. mBio 8:e01415-17. https://doi.org/10.1128/mBio.01415-17.
32. Cleary JD, Chapman SW, Nolan RL. 1992. Pharmacologic modulation of interleukin-1 expression by amphotericin B-stimulated human mononuclear cells. Antimicrob Agents Chemother 36:977–981. https://doi.org/10.1128/AAC.36.5.977.
33. Cleary JD, Weisdorf D, Fletcher CV. 1988. Effect of infusion rate on amphotericin B-associated febrile reactions. Drug Intell Clin Pharm 22:769–772. https://doi.org/10.1177/106002808802201005.
34. Arning M, Kliche KO, Heer-Sonderhoff AH, Wehmeier A. 1995. Infusion-related toxicity of three different amphotericin B formulations and its relation to cytokine plasma levels. Mycoses 38:459–465. https://doi.org/10.1111/j.1439-0507.1995.tb00020.x.
35. Cleary JD, Chapman SW, Swiatlo E, Kramer R. 2007. High purity amphotericin B. J Antimicrob Chemother 60:1331–1340. https://doi.org/10.1093/jac/dkm322.
36. Falk R, Hacham M, Nyska A, Foley JF, Domb AJ, Polacheck I. 2005. Induction of interleukin-1beta, tumour necrosis factor-alpha and apoptosis in mouse organs by amphotericin B is neutralized by conjugation with arabinogalactan. J Antimicrob Chemother 55:713–720. https://doi.org/10.1093/jac/dki090.
37. Radwan MA, AlQuadeib BT, Siller L, Wright MC, Horrocks B. 2017. Oral administration of amphotericin B nanoparticles: antifungal activity, bioavailability and toxicity in rats. Drug Deliv 24:40–50. https://doi.org/10.1080/10717544.2016.1228715.
38. Freeman AF, Stratton P, Swaim D, McManus MT, Darnell D, Urban D, Ferre E, Kim T, Kumar P, Holland S, Kling D, Craft J, Lu R, Mannino R, Lionakis MS, Tramont E. 2015. Oral encochleated amphotericin B (CAMB) in the treatment of chronic azole resistant mucocutaneous candidiasis, abstr. 240. Abstr 115th Gen Meet Am Soc Microbiol. American Society for Microbiology, Washington, DC.
39. Waterman S, Hacham M, Hu G, Zhu X, Park Y, Shin S, Panepinto J, Valyi-Nagy T, Beam C, Husain S, Singh N, Williamson P. 2007. Role of a *CUF1-CTR4* copper regulatory axis in the virulence of *Cryptococcus neoformans*. J Clin Invest 117:794–802. https://doi.org/10.1172/JCI30006.
40. Code of Federal Regulations. 2018. Title 21. Food and drugs. Chapter I. Food and Drug Administration, Department of Health and Human Services. Subchapter A. General. Part 58. Good laboratory practice for nonclinical laboratory studies. 21 CFR 58. https://www.accessdata.fda.gov/scripts/cdrh/cfdocs/cfcfr/CFRSearch.cfm?CFRPart=58&showFR=1.